Exploring fishing impacts on the structure and functioning of the Yellow Sea ecosystem using an individual-based modeling approach

Runlong Sun [a], Peng Sun [a,*], Haiqing Yu [b], Peilong Ju [a], Shuyang Ma [a], Zhenlin Liang [c], Mikko Heino [d, e, f], Yunne-Jai Shin [g], Nicolas Barrier [g], Yongjun Tian [h, i]

[a] Key Laboratory of Mariculture, Ministry of Education, Ocean University of China, Qingdao, China
[b] Institute of Marine Science and Technology, Shandong University, Qingdao, China
[c] Marine College, Shandong University, Weihai, China
[d] Department of Biological Sciences, University of Bergen, Bergen, Norway
[e] Institute of Marine Research, Bergen, Norway
[f] International Institute for Applied Systems Analysis, Laxenburg, Austria
[g] IRD, Univ Montpellier, Ifremer, CNRS, MARBEC, Montpellier, France
[h] Frontiers Science Center for Deep Ocean Multispheres and Earth System (FDOMES), Ocean University of China, Qingdao, China
[i] Laboratory for Marine Fisheries Science and Food Production Processes, Pilot National Laboratory for Marine Science and Technology, Qingdao, China

ABSTRACT

The Yellow Sea is a marginal sea in the Northwestern Pacific where the fishery resources have been overfished and the community structure has greatly changed over the past six decades. Ecosystem modeling approaches are valuable tools to uncover potential mechanisms behind the ecosystem changes. Here, we developed 'OSMOSE YS', an individual-based multispecies OSMOSE model that includes important commercial pelagic and demersal fish and invertebrates in the Yellow Sea. Simulations were carried out under three fishing scenarios to investigate how different levels of fishing pressure may have impacted the Yellow Sea ecosystem. Results indicate that the biomass of demersal fish continued to decline during 1970–2014, while the biomass of pelagic fish and in vertebrates fluctuated periodically. Long-term fishing pressure has led to the reduction of total biomass, body sizes, and longevity of the modelled species. Under low-fishing condition, the ecosystem biomass is restored and the proportion of elder and larger individuals increases. On the contrary, high-fishing condition further decreases the proportion of high-trophic-level species. OSMOSE-YS serves as a baseline model to investigate ecosystem responses to different fishing strategies, in support of ecosystem-based fisheries management in the Yellow Sea.

1. Introduction

The Yellow Sea is a semi-closed marginal sea and one of the most intensely exploited shallow seas in the Northwest Pacific Ocean, providing 10% of the world's population with marine resources, eco nomic opportunities and ecological services (Wang et al., 2016). It also provides important spawning and feeding grounds for many commercially important fish species, such as small yellow croaker (*Larimichthys polyactis*), largehead hairtail (*Trichiurus japonicus*), Japanese Spanish mackerel (*Scomberomorus niphonius*), and Japanese anchovy (*Engraulis japonicus*) (Jin, 2003). However, since the 1980s, overexploitation has led to large changes in the fish community structure and diversity, and the functioning of food webs (Jin and Tang, 1996; Shen and Heino, 2014; Szuwalski et al., 2020). In particular, fishing has been selectively removing larger individuals or higher trophic levels species resulting in the reduction of fish size and of the biomass of vulnerable species (Xu and Jin, 2005; Li et al., 2021). The situation observed in Yellow Sea fisheries is consistent with the global phenomenon known as "fishing down the food web", as large, high-trophic-level species are caught or removed from the ecosystem faster than they are replenished, leading to an increase in the proportion of low-trophic-level species, which ultimately manifests itself as a continuing decline in the mean trophic level of fishery landings (Pauly et al., 1998; Pauly and Watson, 2005). With the increase of fishing vessels and their power in the Yellow Sea, combined with the modernization of fishing gears and methods, commercially important, long-lived piscivorous fish have been replaced by low value, short-lived planktivorous fish, resulting in the reduction of fishery production (Tang et al., 2016). Therefore, developing sustainable fisheries in the Yellow Sea in the context of ecosystem-based management is urgent, a task that can be assisted by utilizing suitable ecological indicators to investigate the impact of fishing pressure (Tang et al., 2016; Li et al., 2021).

The aim of ecosystem-based fishery management (EBFM) is to ensure both a healthy marine ecosystem and the sustainable development of fisheries (Pikitch et al., 2004). By taking into account multiple biotic and abiotic factors and their interactions within the ecosystem, EBFM adopts an integrated approach to fisheries management in the ecological realm, aiming to balance different societal goals and illuminate tradeoffs among ecosystem services and fishery management objectives (FAO, 2008; Levin et al., 2009). As the dynamics of marine ecosystems can be more complicated than one would expect, traditional single-species models, which ignore the many ecological interactions inherent in complex marine ecosystems, have some important limitations (Garcia et al., 2003; Plagányi, 2007; Szuwalski et al., 2017). Multispecies and ecotrophic ecosystem models have been developed to address complex ecosystem interactions and their effects, and they have been applied worldwide in support of the EBFM goals. Ecosystem models aim to represent the entire ecological system (Fulton, 2010), its spatial structure, the many biotic and abiotic components and their interactions, by accounting for ecosystem-level uncertainties (Seidl, 2017; Pikitch et al., 2004). Examples of such ecosystem models include EwE (Ecopath with Ecosim; Christensen and Walters, 2004), Atlantis (Atlantis Ecosystem Model; Fulton et

al., 2004), and OSMOSE (Object-oriented Simulator of Marine ecoSystem Exploitation; Shin and Cury, 2001, 2004). Recently, Ecopath models were developed in the southern Yellow Sea to explore trophic interactions, ecosystem structure and energy flows in the ecosystem (Lin et al., 2013). A few other ecosystem models were also built for the Yellow Sea, including an Ecopath model for an artificial reef zone of the Lidao ecosystem and an Ecopath model as well as an OSMOSE model for the semi-enclosed Jiaozhou Bay (Wu et al., 2016; Xing et al., 2017; Ma et al., 2018). These ecosystem models for the Yellow Sea were developed in relatively small areas and focused largely on model parameterization, trophic levels of functional groups, and food web structure. But while there has been abundant modeling of food web and multispecies communities within Yellow Sea ecosystems, there remains a gap in modeling the ecological dynamics at the scale of the large marine ecosystem, which is modeling that accounts for the complexity of species introductions, multispecies interactions and spatial dynamics in the Yellow Sea ecosystem.

The reason for choosing OSMOSE as a tool in this study is to exploit the characteristics of the individual-based model to study the impacts of different fishing pressure on the ecosystem from the perspective of the life history cycle process of key species in the ecosystem and the trophic interactions based on the size of individuals, and also because of the fishery characteristics of the Yellow Sea ecosystem where there is a relative lack of data. OSMOSE and Ecopath models are quite different in both their structure and assumptions (Christensen and Walters, 2004; Shin and Cury, 2001, 2004). In particular, diets in OSMOSE emerge from size-based processes, while diets reconstructed from empirical data are input into Ecopath. And Atlantis model is considered one of the best ecological modeling frameworks worldwide for the simulation of fishing scenarios but is more suitable for data-rich study areas due to its rich sub-models and the large amount of parameter information required (Plagányi, 2007).

The application of OSMOSE model in the Yellow Sea provides different perspectives on the functioning of the Yellow Sea ecosystem, while being able to understand the ecosystem dynamics and fishing effects. OSMOSE is a spatially-explicit individual-based multispecies model that explicitly simulates the dynamics of modelled species and their interactions to understand the functioning of marine food webs and to explore hypotheses about the mechanisms underlying ecosystem resilience (Shin and Cury, 2001, 2004). OSMOSE has been widely used in various marine ecosystems around the world to investigate fishing effects, exploring their spatial and trophic dynamics, the impacts of climate change and their implication for fisheries management (Shin and Cury, 2004; Fu et al., 2013, 2017; Travers-Trolet et al., 2014; Grüss et al., 2015; Moullec et al., 2019a; Guo et al., 2019).

Ecological indicators have been widely used to study the impacts of various driving factors on ecosystems and can provide guidance for ecosystem-based fisheries management and ecosystem restoration (Fu et al., 2017; Thompson et al., 2020). Selecting appropriate ecological indicators to represent the state of ecosystems has become an important research focus in the past two decades (e.g., Shin et al., 2010; Otto et al., 2018). The applicability of ecological indicators for studying fish community structure in the Yellow Sea has already been demonstrated (Li et al., 2021). Assessing the impact of fishing on an ecosystem using ecological indicators needs to account for specific ecosystem features and fishing history (Shin et al., 2018). The Yellow Sea ecosystem has been under high fishing pressure for a long period, thus the changes of ecological indicators in this study reflected the changes of the Yellow Sea ecosystem under long-term fishing pressure. Previous studies have compared the changes of ecological indicators under multiple scenarios to study the effects of fishing and climate change on ecosystems (Fu et al., 2013; Shin et al., 2018; Fu et al., 2020). In this study, we focused on the long-term changes of these ecological indicators, particularly addressing regime shifts.

In this study, an OSMOSE model for the Yellow Sea (hereafter referred to as OSMOSE-YS) was applied to explore the ecosystem dynamics, fishing effects, and balanced harvest strategies in this ecosystem (Sun et al., 2023). Using the OSMOSE-YS model, we aim to investigate the effects of fishing pressure on the Yellow Sea ecosystem by simulating long-term changes in total biomass, yield, and size and age structure of modelled species, and ecological indicators at the ecosystem level. Three scenarios of fishing mortality rates were experimented to reveal how different levels of fishing pressure might have impacted the Yellow Sea at both species and ecosystem levels.

2. Material and methods

2.1. Study area and OSMOSE model components

The Yellow Sea is located in the Northwest Pacific Ocean, covering a total area of about 400,000 km^2 with an average water depth of 44 m (Yang et al., 2003; Zhang et al., 2016). The grid of the OSMOSE-YS model has a spatial resolution of 10×10 km^2 (Fig. 1). The northwest and southern boundaries of the study area are based on the actual Yel low Sea area, while the eastern boundary is 126°E (Fig. 1).

OSMOSE is a two-dimensional, multi-species and individual-based model which is spatially explicit and represents the whole lifecycle of interacting marine modelled species. The modelled processes of the lifecycle are from eggs to adult fish and species interact through pre dation in a spatial and dynamic way (Shin and Cury, 2001, 2004). We focus on 13 species in the OSMOSE-YS model: Japanese anchovy (*Engraulis japonicus*), chub mackerel (*Scomber japonicus*), Japanese Spanish mackerel (*Scomberomorus niphonius*), silver pomfret (i), largehead hairtail (*Trichiurus lepturus*), small yellow croaker (*Larimichthys polyactis*), Pacific cod (*Gadus microcephalus*), yellow striped flounder (*Pseudopleuronectes herzensteini*), Pacific sandlance (*Ammodytes personatus*), South American pilchard

(*Sardinops sagax*), southern rough shrimp (*Trachysalambria curvirostris*), Japanese flying squid (*Todarodes pacificus*), and swimming crab (*Portunus trituberculatus*). These 13 species are typically regarded as important components of the Yellow Sea marine ecosystem due to their large contribution to the total biomass and their high economic value (Tang et al., 2016).

The life cycle of each modelled species from egg to terminal age is simulated at a time step of three months. The total number of eggs of each species is split into 120 super-individuals (referred to as "schools"). Individuals of a school share the same body length, age, food requirement and spatial coordinates at a given time step and are distributed spatially according to distribution maps. The distribution maps of each species are density-based and obtained from georeferenced data of research surveys (Tang et al., 2016).

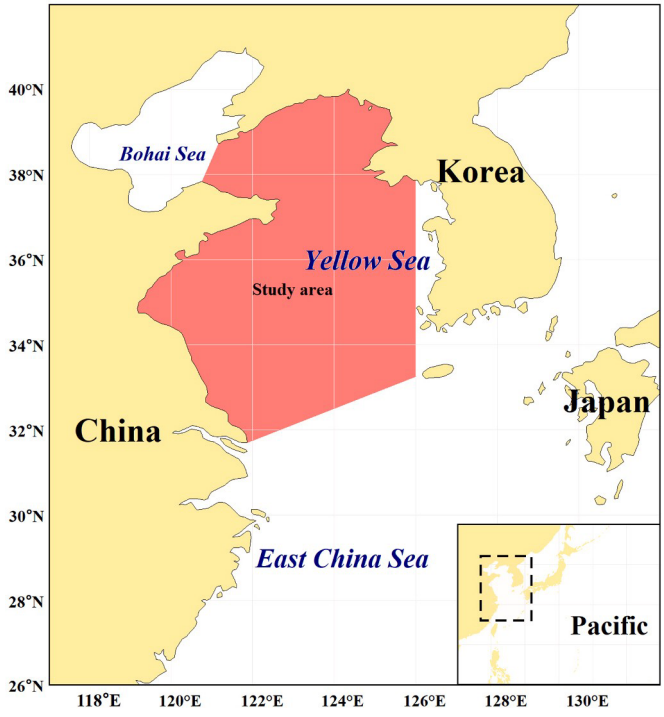

Fig. 1. Study area for the OSMOSE-YS model in the Yellow Sea.

At each time step, OSMOSE simulates biological and ecological processes, including growth, predation, starvation, fishing, reproduction, spatial movement, and diverse natural mortality due to causes unaccounted for by the model (Fu et al., 2017). At each time step, schools move randomly in their habitat to an adjacent cell based on the probability of movement that is given by fish density map. The average growth of the schools follows the von Bertalanffy growth model, and individual growth variability is determined by consumption rate and prey availability (Shin and Cury, 2004). Two groups of phytoplankton and zooplankton, whose biomasses were derived from a calibrated biogeochemical model (i.e., FVCOM-NEMURO; Xing et al., 2017, Yu et al., 2020), are included in the OSMOSE-YS model as food sources for individuals and species at lower trophic levels. The phytoplankton and zooplankton groups and the 13 modelled species are linked through trophic interactions to represent the range of food webs in the Yellow Sea fisheries ecosystem from plankton to economic fishery species.

At the end of each time step, reproduction occurs for schools achieving sexual maturity, producing eggs proportional to the spawning stock biomass, sex ratio, relative annual fecundity, and spawning seasonality (Fu et al., 2013; Travers-Trolet et al., 2014). All biological parameters that are input into the model in relation to growth, mortality, and reproduction are provided in Table S1.

The OSMOSE-YS model explicitly considers different sources of mortality. Fishing mortality is applied to exploited schools that reach the age or size of recruitment to the fishery, which is assumed to be uniform over space. Both predation mortality and starvation mortality depend on prey availability. Predation is assumed to be opportunistic and size based, depending on the size ratio between prey and predators and their spatiotemporal cooccurrence, while the growth in size and weight of individuals is determined based on their predation success (Fu et al., 2013). Small individuals are susceptible to top-down predator regulation, whereas large individuals are regulated by bottom-up food avail ability. Minimum and maximum predator/prey size ratios are computed based on diet research when available, or derived from observed diets and species' mean sizes (Froese and Pauly, 2010). Larval mortality ap plies to the period from eggs to first feeding larvae. Diverse natural mortality in OSMOSE-YS includes all types of mortality that are unaccounted for in the model, which was estimated from previous studies (Froese and Pauly, 2010; Table S1). Mean trophic level predicted by OSMOSE emerge from size-based trophic interactions, and $TL = \sum_i Tl_i\ B_i/B$, where Tl_i represents the trophic level of fish school i, B_i represents the biomass of fish school i for a species, B represents the total

biomass of a species (Travers et al., 2010; Grüss et al., 2015; Xing et al., 2017).

OSMOSE-YS was calibrated to constrain predicted biomass and yield of modelled species within realistic ranges. An evolutionary algorithm (EA), which has been developed for the calibration of complex stochastic models, was used to calibrate OSMOSE-YS (Duboz et al., 2010; OliverosRamos and Shin, 2016) The evolutionary algorithm has been widely used to calibrate ecosystem models (e.g., OliverosRamos et al., 2017; Moullec et al., 2019b; Grüss et al., 2015; Halouani et al., 2016). The unknown parameters for each modelled species were estimated through the model calibration by fitting the simulated biomass and yield of a specific species to observed data using maximum likelihood objective functions (OliverosRamos et al., 2017). The calibration process of OSMOSE-YS allowed us to estimate unknown parameters and the unknown parameters estimated in the OSMOSE-YS model for each species included coefficients of plankton accessibility to the modelled species, larval mortality (mortality of eggs and 0–1 month old individuals), and catchability index (Table S2). The catchability index was used to scale the OSMOSE-YS model outputs to account for the availability of modelled species to fishing gears. The calibration process used the 'calibraR' (https://cran.rproject.org/web/packages/calibrar) R packages (Oliveros-Ramos et al., 2017; Oliveros-Ramos and Shin, 2016). Observed yield data for the period 1970–2014 in the Yellow Sea were obtained from the Sea Around Us project (Pauly and Zeller, 2016) and the observed biomass data were estimated by the optimized catch-only method (OCOM; Zhou et al., 2018), which has been used to estimate management quantities across a range of stocks simultaneously (Table S3). OCOM is mainly based on a Graham-Schaefer surplus pro duction model to estimate biomass, which may cause potentially estimation uncertainties in the calibration process (Zhou et al., 2017; Zhou et al., 2018). When the biological parameters and target reference data are reliable, the estimated parameters can be considered reliable and ecologically meaningful. Otherwise, these parameters involved in the calibration process are only used as calibration parameters to ensure that the biomass and yield levels in OSMOSE-YS match the observed levels (Grüss et al., 2015). The stochasticity of OSMOSE-YS mainly comes from the distribution of schools over space using density maps, the implementation of random walk movements and the order of schools interaction through predation.

2.2. *Estimation of fishing pressure and simulation scenarios*

With the calibrated OSMOSE-YS model, the long-term effects of fishing pressure in the Yellow Sea were investigated. Since time series of fishing mortality rates from stock assessments are unavailable for the modelled species, we introduced the process of standardizing the time series of engine power of fishing vessels (obtained from the Chinese Fishery Statistics, Zhao et al., 2020) to approximate the variation of fishing pressure in the Yellow Sea ecosystem. The biomass estimates by the OCOM, as well as the available yield data were used in the calibration process, i.e. as an independent data source and only as a reference for the process of convergence of the model results. Although these two parameters can also calculate fishing mortality rates for the time series, to avoid the effects of using reference data as inputs to the model results, we used the engine power of Chinese marine fishing vessels. The total engine power of marine fishing vessels in the Yellow Sea at time t, P_t, was calculated as:

$$P_t = \sum_p Y_{p,t}^{YS} / Y_{p,t} \; P_{p,t}$$

where the summation is over eight provinces ($p \in$ Tianjin, Hebei, Liaoning, Shanghai, Jiangsu, Zhejiang, Fujian, and Shandong), $Y_{p,t}^{YS}$ and $Y_{p,t}$ are the marine fisheries catch by vessels registered in province p at time t in the Yellow Sea and in all Chinese Seas (Bohai Sea, Yellow Sea, East China Sea, and South China Sea), respectively, and, $P_{p,t}$ is the total engine power of marine fishing vessels registered in province p at time t (Table S4).

The total power of fishing vessels was standardized to reflect the annual variability of fishing effort:

$$P_i^{sta} = \frac{P_t - P_{mean}}{P_{stdev}}$$

where P_{i}^{sta} is the standardized fishing vessel power at time t, and P_{mean} and P_{stdev} are the mean and standard error of P_t.

Furthermore, we used standardized fishing vessel power as a proxy for fishing mortality variations over time (Table S4). Annual fishing mortality rate was then calculated as:

$$F_t = F_b e^{\delta P_i^{sta}}$$

where F_t is the fishing mortality rate at time t, F_b is the baseline fishing mortality rate estimated from previous studies, and δ is a parameter that determines the degree of fishing impact from fishing vessel power. We hypothesized that the annual fishing mortality rates were correlated with the fishing vessel power, and the δ value reflected the degree of variability in fishing mortality in the study area (set to 0.1 in this study based on calculating the lowest relative difference repeatedly). That was, the fishing capacity was used as a proxy of fishing pressure, assuming that spatial and temporal allocation of this degree of variability did not vary among different years. Although this approach only

considered Chinese fishery data, which may not be used as an indicator of changes in fishing mortality in the whole Yellow Sea, but it is consistent with species modeling and fishing scenario setting in this study, and is able to capture indicators of changes in fishing pressure to reflect ecosystem responses.

Using the calibrated OSMOSE-YS, we simulated ecosystem dynamics under three fishing scenarios to explore the impacts of varying fishing pressure: (1) historical baseline condition under the historical fishing mortality rates (a scenario denoted as F1); (2) low-fishing condition: halving the baseline fishing mortality rates (denoted as F0.5); (3) high fishing condition:1.5 times the baseline fishing mortality rates (denoted as F1.5).

The OSMOSE-YS model was run for 100 years to ensure that the biomass and yield of the modelled species reach steady state; the simulation outputs of the last 45 years (1970–2014) were used for further analyses. In the OSMOSE-YS model, the dynamics of these 13 modelled species start with their initial biomass, which were obtained from OCOM (Pauly and Zeller, 2016; Zhou et al., 2018). As OSMOSE is a stochastic model, the simulation scenarios in OSMOSE-YS were repeated 100 times and outputs were averaged over the 100 simulations.

2.3. *Ecological indicators*

To investigate the impact of fishing pressure on the structure and function of the ecosystem, we employed five types of ecological indicators refer to existing studies applying OSMOSE (Fu et al., 2020), based on the OSMOSE-YS model outputs: (1) biomass-based, (2) yield based, (3) size-based, (4) age-based, and (5) trophic-based indicators. Specifically, biomass-based indicators include the total fish biomass of all-trophic-level species (*B*), biomass of lower-trophic-level species (*B_LTL*: the biomass at trophic levels $\leq$3.25), and biomass of higher trophic-level species (*B_HTL*: the biomass at trophic levels >3.25).

Yield-based indicators include the total yield of all species (Y) and biomass-to-yield ratio (B/Y). Size-based indicators include the proportion of fish larger than 20 cm (Large Fish Indicator LFI20), the proportion of fish larger than 40 cm (LFI40), and in the fisheries catch, the proportion of fish larger than 20 cm (LCI20), and the proportion of fish larger than 40 cm (LCI40). Age-based indicators include the proportion of fish older than 2 years (AO2) and the proportion of fish older than 4 years (AO4). Trophic-based indicators include the mean trophic level of the community (TL) and the ratio of B_LTL to B_HTL (L2H).

The trends and step changes of the ecological indicators under the baseline condition were analyzed using a sequential *t*-test analysis of regime shifts (STARS; Rodionov, 2004). Regime shifts are abrupt, substantial, and persistent changes in the state of natural systems driven by a combination of multiple factors. (Ma et al., 2019; Ma et al., 2020); in this study, we mainly considered those related to fishing pressure. The STARS results were determined by the cutoff length (set to 10 in this study) for the proposed regimes, and the Huber weight parameter (set to 1 in this study) which defines the range of departure from the observed mean, beyond which observations are considered as outliers.

3. Results

3.1. *Species biomass and yield*

Using the evolutionary algorithm, the OSMOSE-YS model was calibrated so that the simulated yields of most modelled species under the baseline condition (Scenario F1) were in the acceptable intervals (minimum and maximum values of the observed yields) and the simulated biomass order among modelled species was consistent with the biomass estimated by OCOM (Figs. S1, S2). Temporal patterns of simulated biomass varied by species. Pelagic and invertebrate species were relatively stable during the whole period (Fig. 2A, C). The biomass of Japanese anchovy gradually increased from 349 to 400 thousand tons after the 1990s. Swimming crab had the highest biomass among invertebrate species, showing a stable fluctuation trend (Fig. 2C). By contrast, the biomass of demersal fish species showed a generally stable trend in the 1970s and a subsequent declining trend from the 1970s to 2010s (Fig. 2B). The biomass of largehead hairtail was the highest in the 1970s but had decreased from 450 to 350 thousand tons by 2014. The biomass of yellow striped flounder decreased the most from 150 to 6.7 thousand tons by 2014, while the biomass of Pacific cod decreased from 90 to 14 thousand tons. The biomass of small yellow croaker was relatively stable during the whole period, fluctuating around 30 thousand tons (Fig. 2B). The yields of pelagic and invertebrate species were stable before 1990s but gradually increased from the 1990s to the 2010s, with the exception of Japanese Spanish mackerel and Japanese flying squid, whose yields fluctuated around 7 and 20 thousand tons, respectively (Fig. 2D, E, F). In particular, the yield of Japanese anchovy increased from 32 to 51 thousand tons (Fig. 2D). However, the yields of most demersal fish species show a slightly decreasing trend after 1990s, except for yellow striped flounder and Pacific cod, which showed strong declines in yield (Fig. 2E). The yield of largehead hairtail increased from 80 to 90 thousand tons, while that of small yellow croaker doubled from 40 to 90 thousand tons by 2014 (Fig. 2E).

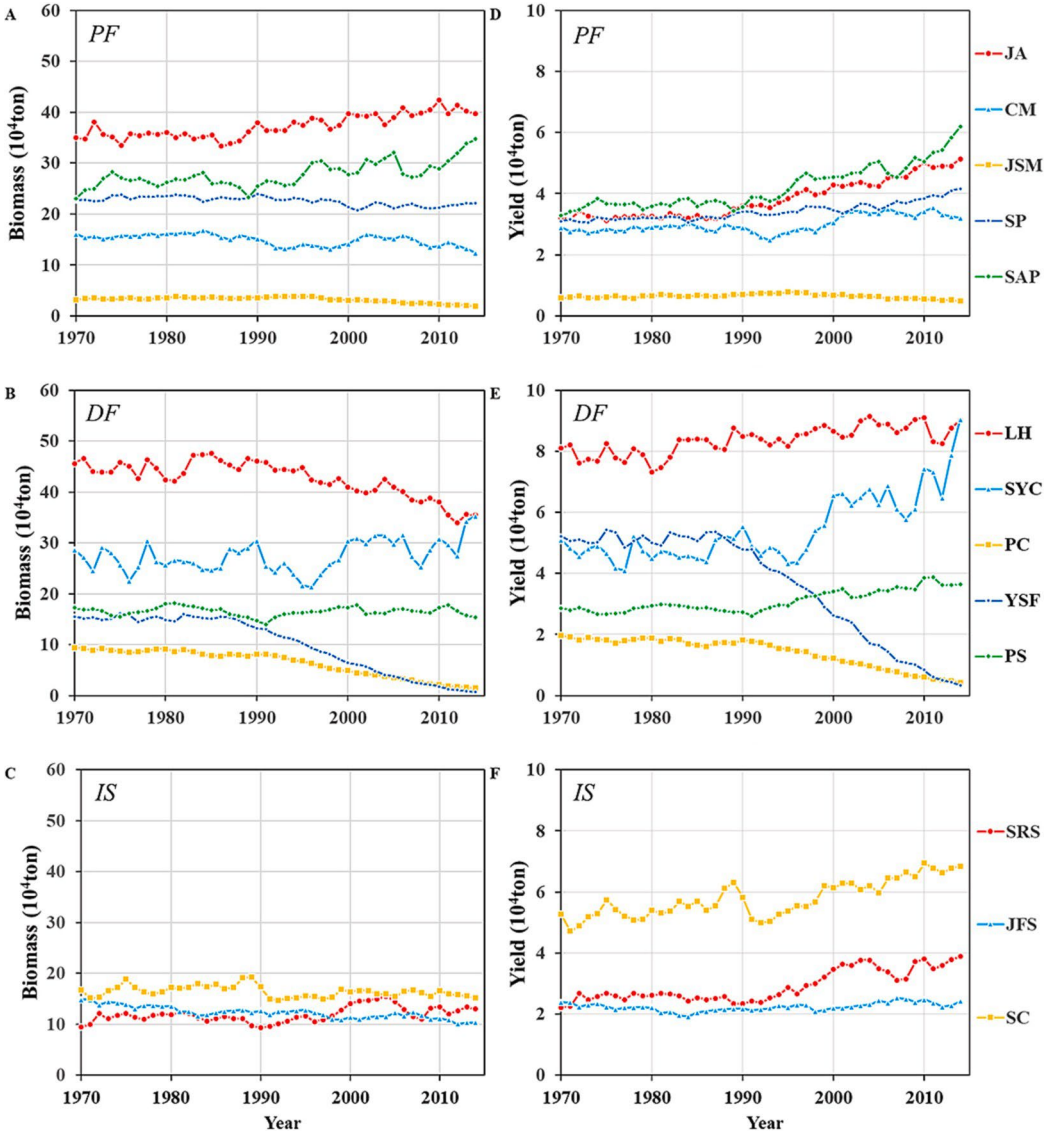

Fig. 2. The simulated biomasses (AC) and yields (D—F) of the 13 species modelled during 45 years of simulation in OSMOSE-YS (*F1* scenario). The simulated data are averages of 100 replicates. Top row: pelagic fish species (*PF*), middle row: demersal fish species (*DF*), bottom row: invertebrate species (*IS*). JA: Japanese anchovy (*Engraulis japonicus*), CM: Pacific chub mackerel (*Scomber japonicus*), JSM: Japanese Spanish mackerel (*Scomberomorus niphonius*), SP: Silver pomfrets (*Pampus argenteus*), LH: Largehead hairtail (*Trichiurus lepturus*), SYC: Small yellow croaker (*Larimichthys polyactis*), PC: Pacific cod (*Gadus microcephalus*), YSF: Yellow striped flounder (*Pseudopleuronectes herzensteini*), PS: Pacific sandlance (*Ammodytes personatus*), SAP: South American pilchard (*Sardinops sagax*), SRS: Southern rough shrimp (*Trachysalambria curvirostris*), JFS: Japanese flying squid (*Todarodes pacificus*), SC: Swimming crab (*Portunus trituberculatus*). For interquartile ranges, see Figs. S3 & S4.

3.2. Size and age structure and mean trophic level under fishing scenarios

The changes in size structure according to changes in fishing mortality varied among species (Fig. 3). The proportions of small individuals for Japanese anchovy, south American pilchard and southern rough shrimp under high-fishing condition were higher than those under low fishing condition (Fig. 3A, J, K). For the other 10 species, the proportions of small individuals were higher under low-fishing condition or stable (Fig. 3B, C). For yellow striped flounder, Pacific sandlance and Japanese flying squid, the proportions of small individuals exceeded 70% under low-fishing condition (Fig. 3H, I, L).

The age structure under the three fishing scenarios was relatively stable for most species (Fig. 4). Japanese anchovy, small yellow croaker and yellow striped flounder had lower proportions of young fish (age<2) under high-fishing condition than under low-fishing condition, while the proportions of young individuals for chub mackerel, Pacific sand lance and swimming crab under high-fishing condition were higher than those under low-fishing condition (Fig. 4A, C, F, H, I, M). Interestingly, because of changes in somatic growth, for some species the trends in age and size structure were opposite; in the case of the Japanese anchovy, for example, there is a significant decrease of the mean length at age with fishing intensity.

The overall trophic level structure of simulated species was relatively stable, and there was no significant difference under the three fishing scenarios (Fig. 5). However, there was a slight tendency for the mean trophic level to increase with higher fishing condition for low trophic species, whereas the opposite tendency was recorded for the species with the highest trophic level (Japanese Spanish mackerel and chub mackerel).

3.3. Changes in ecological indicators

Under baseline fishing condition, the ecological indicators generally showed decadal variations (Fig. 6). All biomass-based indicators, with the exception of *B_LTL* (the biomass of lower-trophic-level species), showed a clear long-term decreasing trend (Fig. 6A–D). The total biomass of the ecosystem continuously decreased from the late 1980s to 2010s with two step changes (1990/1991 and 2006/2007). Meanwhile, the total yield increased drastically from the late 1990s, with step changes that were consistent with the total biomass (Fig. 6D). The biomass-to-yield ratio showed decreasing trend from 1970s to 2010s with three step changes (1985/1986, 1995/1996, and 2005/2006; Fig. 6E). Among the biomass-based indicators, *B_LTL* was higher than *B_HTL* (the biomass of higher-trophic-level species), and the decline of *B_HTL* was much greater (Fig. 6B, C). While *B_LTL* fluctuated without a clear trend (Fig. 6B), *B_HTL* decreased from 1026 to 830 thousand tons during the simulation period with two step changes (1991/1992 and 2006/2007; Fig. 6C).

All size-based indicators showed decadal variations (Fig. 6F–I). Both LFI20 and LCI20 showed decreasing trends; however, step changes occurred in 1993/1994 and 2008/2009 for the former but only in 2008/ 2009 for the latter (Fig. 6F, G). Similarly, both LFI40 and LCI40 showed downward trends with the same step changes occurring in 1986/1987, 1996/1997 and 2007/2008 (Fig. 6H, I). Regarding age-based indicators, the proportion of fish older than 2 years AO2 was relatively stable during the 1970s–1990s and decreased rapidly after 1990, while AO4 showed a continuously decreasing trend during the whole simulation (Fig. 6J, K). The mean trophic level of the community fluctuated before the 1990s but showed an upward trend during the 2000s–2010s (Fig. 6L). The B_LTL to B_HTL ratio increased after the late 1980s with step changes occurring in 1993/1994 and 2006/2007 (Fig. 6M).

Compared to the baseline fishing condition, ecological indicators under low and high-fishing conditions showed contrasting variation trends (Fig. 7). Using augmented Dickey-Fuller test (ADF test), all ecological indicators were tested for stationarity, and most indicators (except LCI 40, LFI20, AO4 under F0.5, and B_LTL under F1.5) under all three scenarios were nonstationary (Table S5). While the trends of most indicators under high-fishing condition were relatively consistent with those under the baseline condition, those under low-fishing condition fluctuated drastically. The total biomass increased rapidly prior to 1976 under the low-fishing condition but afterwards maintained a continuous downward trend under all three scenarios (Fig. 7A). In contrast, B_LTL showed an upward trend before 1980 and then fluctuated under high fishing condition (Fig. 7B). B_HTL showed a downward trend after 1980 similar to the trends of total biomass under all three scenarios (Fig. 7C, D). The Y was relatively stable but significantly differed under three fishing scenarios (Fig. 7D). The B/Y under low-fishing condition was about 10 with a decreasing trend, while that under high-fishing condition fluctuated around 3.5 (Fig. 7E). Size-based and age-based indicators showed similar trends under the same fishing condition, but there were great differences between different fishing scenarios (Fig. 7F–K). These two types of indicators under the baseline condition showed a continuous downward trend; same was true under high-fishing condition but with a steeper slope. However, under low-fishing condition, size-based and age-based indicators showed an obvious upward trend before 1980, then size-based indicators stabilized while age-based indicators slightly decreased afterwards. The mean trophic level under low-fishing condition showed a sharp decline, fluctuating after 1980 (Fig. 7L). Under high-fishing condition, TL rose continuously until 1990 and then declined rapidly, while TL under baseline condition showed a steady fluctuating upward trend (Fig. 7L). The L2H (the ratio of B_LTL to B_HTL) continued to rise after 1980 under the high fishing condition, while showed slightly increase under baseline and low-fishing conditions (Fig. 7M).

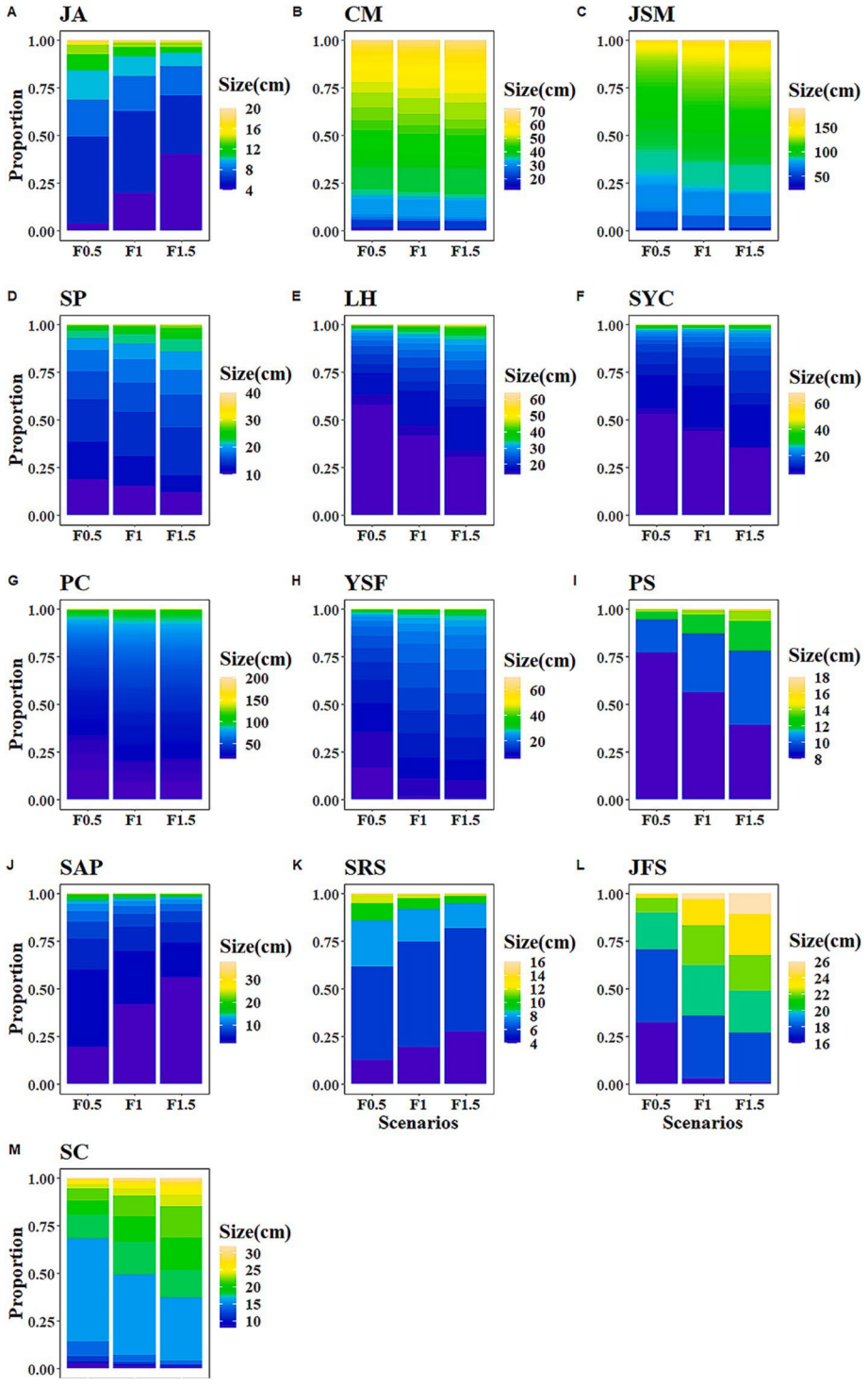

Fig. 3. An interspecies comparison of the size structures under three fishing pressure scenarios (*F0.5*, *F1*, and *F1.5*) in OSMOSE-YS. The size structures are averages of the last 45 years of the simulations. For species codes, see Fig. 2.

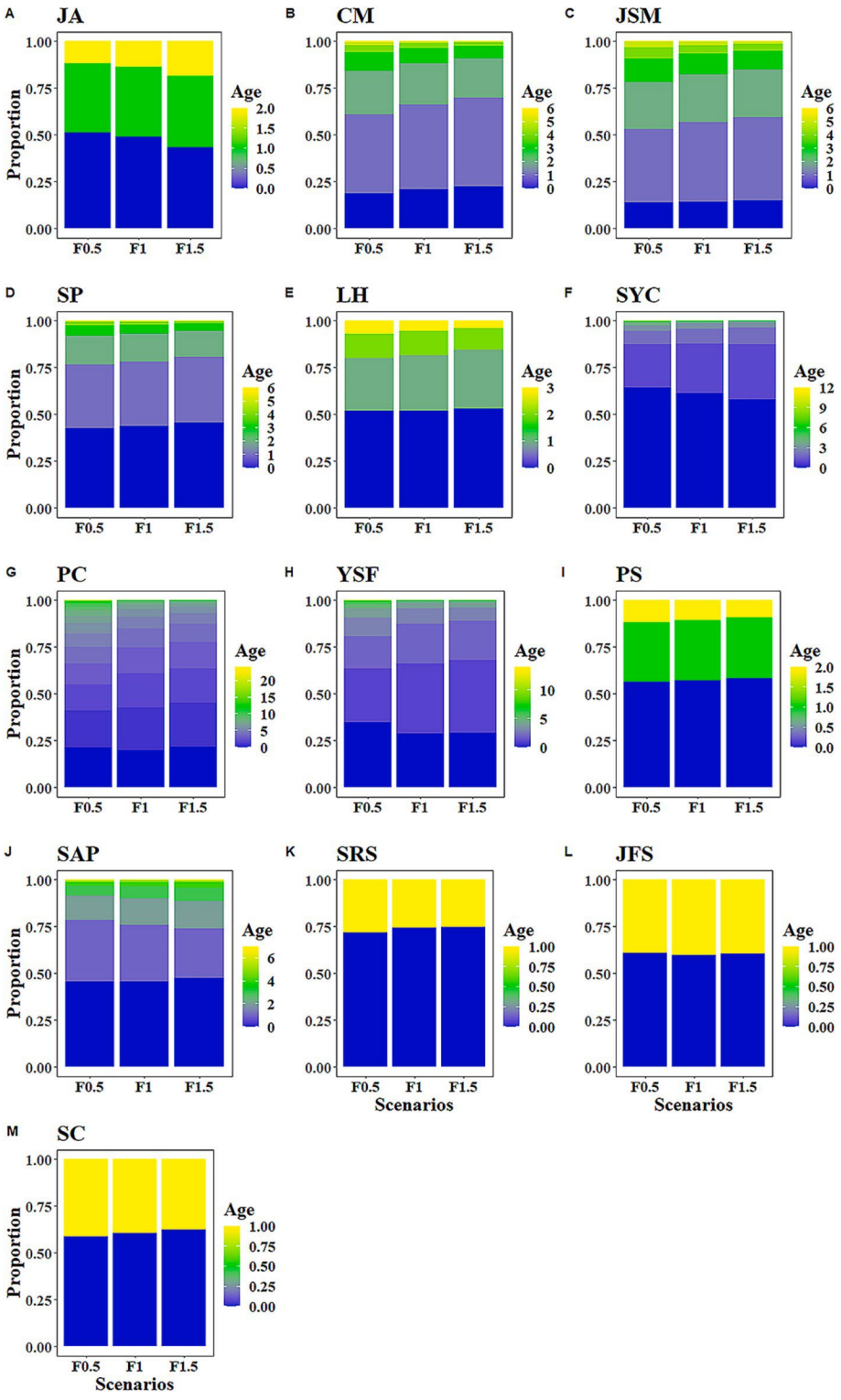

Fig. 4. An interspecies comparison of the age structures under three fishing pressure scenarios (*F0.5*, *F1*, and *F1.5*) in OSMOSE-YS. The age structures are averages of the last 45 years of the simulations. For species codes, see Fig. 2.

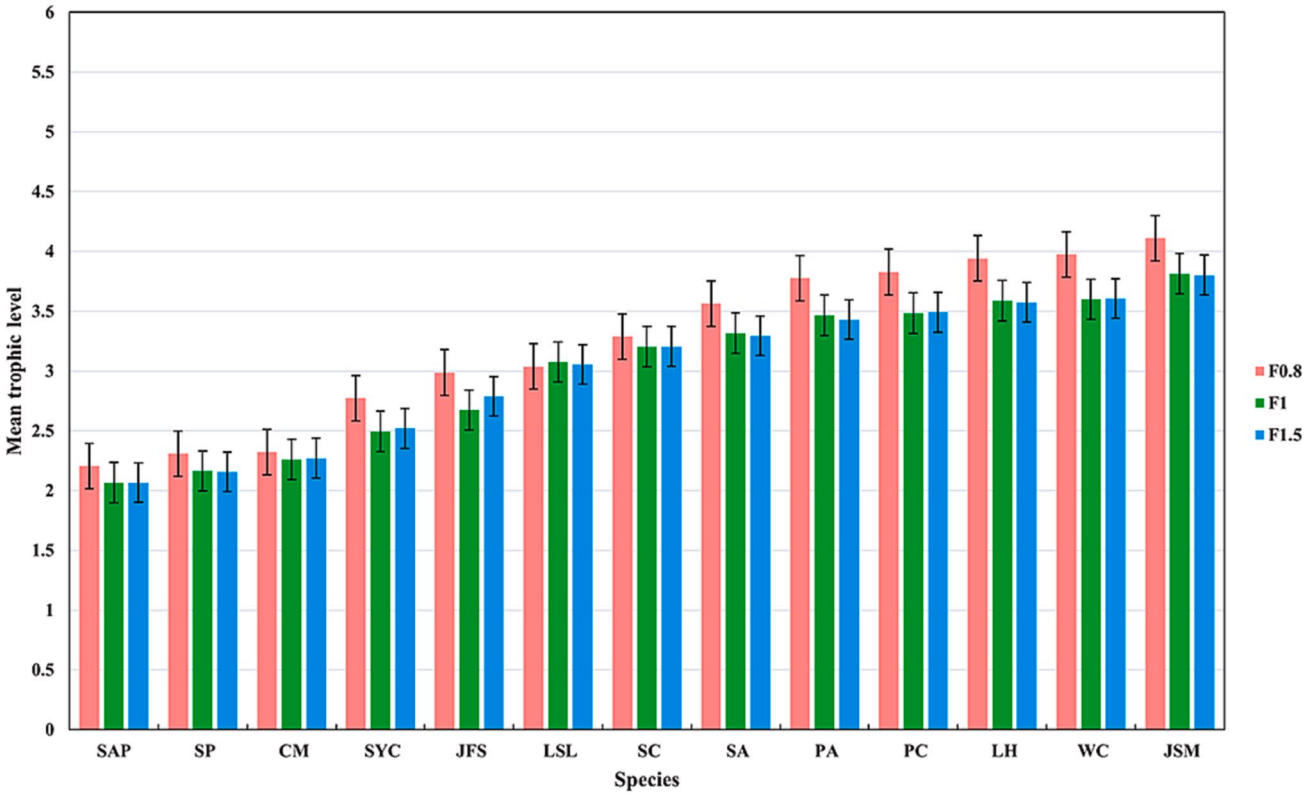

Fig. 5. Mean trophic levels of modelled species under three fishing pressure scenarios (*F0.5*, *F1*, and *F1.5*) in OSMOSE-YS. The trophic levels are averages of the last 45 years of the simulations. For species codes, see Fig. 2.

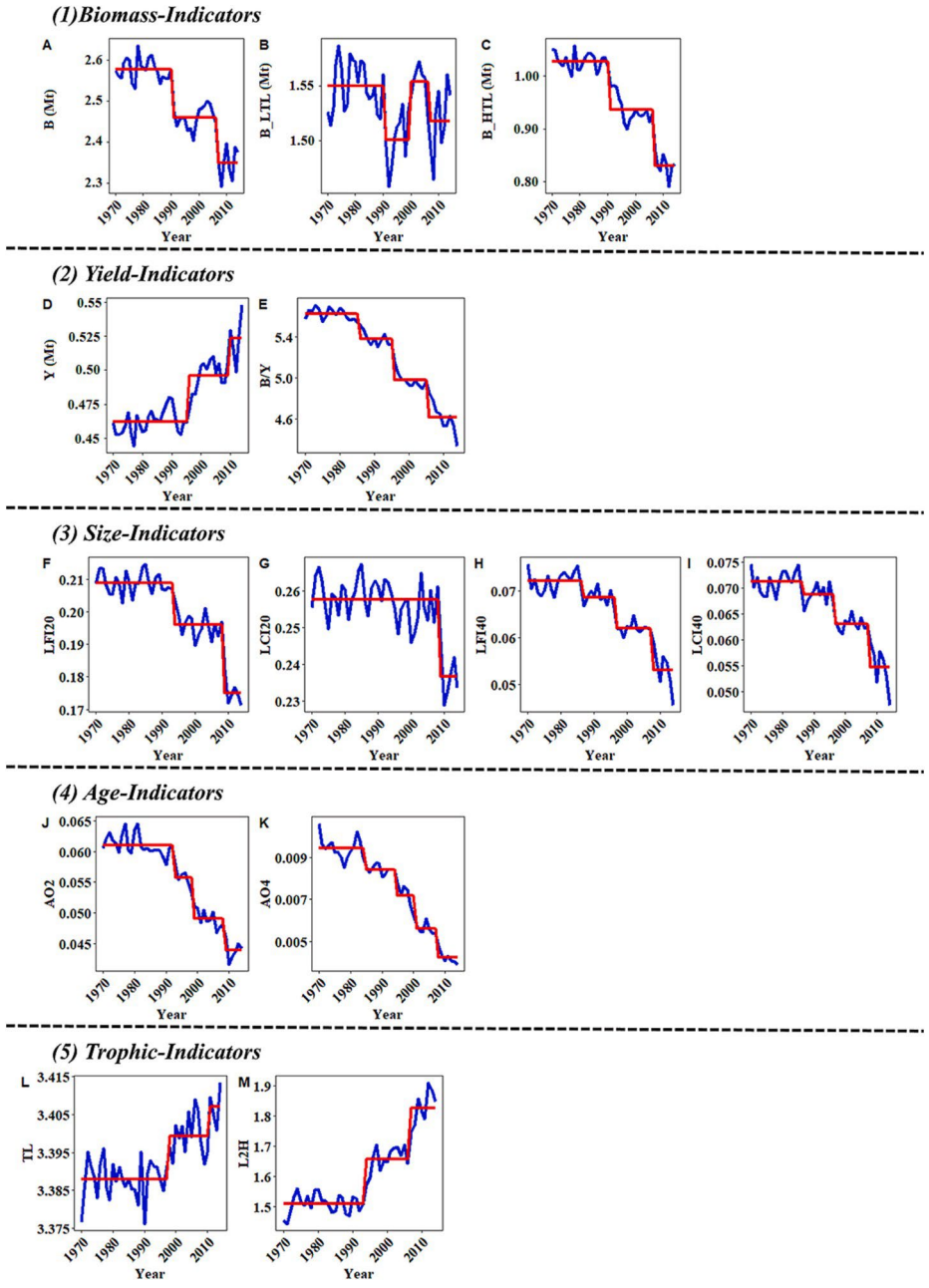

Fig. 6. Changes in ecological indicators during 45 years of simulation in OSMOSE-YS under the baseline fishing scenario (*F1*). The blue lines are the ecological indicators and the red lines indicate regime means detected by regime shift detection methods. *B*: the total biomass of all species, *Y*: the total yield of all species, *B_LTL*: biomass of lower-trophic-level species, *B_HTL*: biomass of higher-trophic-level species, *LFI20*: proportion of large fish (>20 cm) indicator, *LFI40*: proportion of large fish (>40 cm) indicator, *LCI20*: proportion of large catch (>20 cm) indicator, *LCI40*: proportion of large catch (>40 cm) indicator, *AO2*: proportions of fish AGE > 2, *AO4*: proportions of fish AGE > 4, *TL*: mean trophic level of the community, *B/Y*: biomass to fisheries yield ratio, *B_L2H*: ratio of *B_LTL* to *B_HTL*.

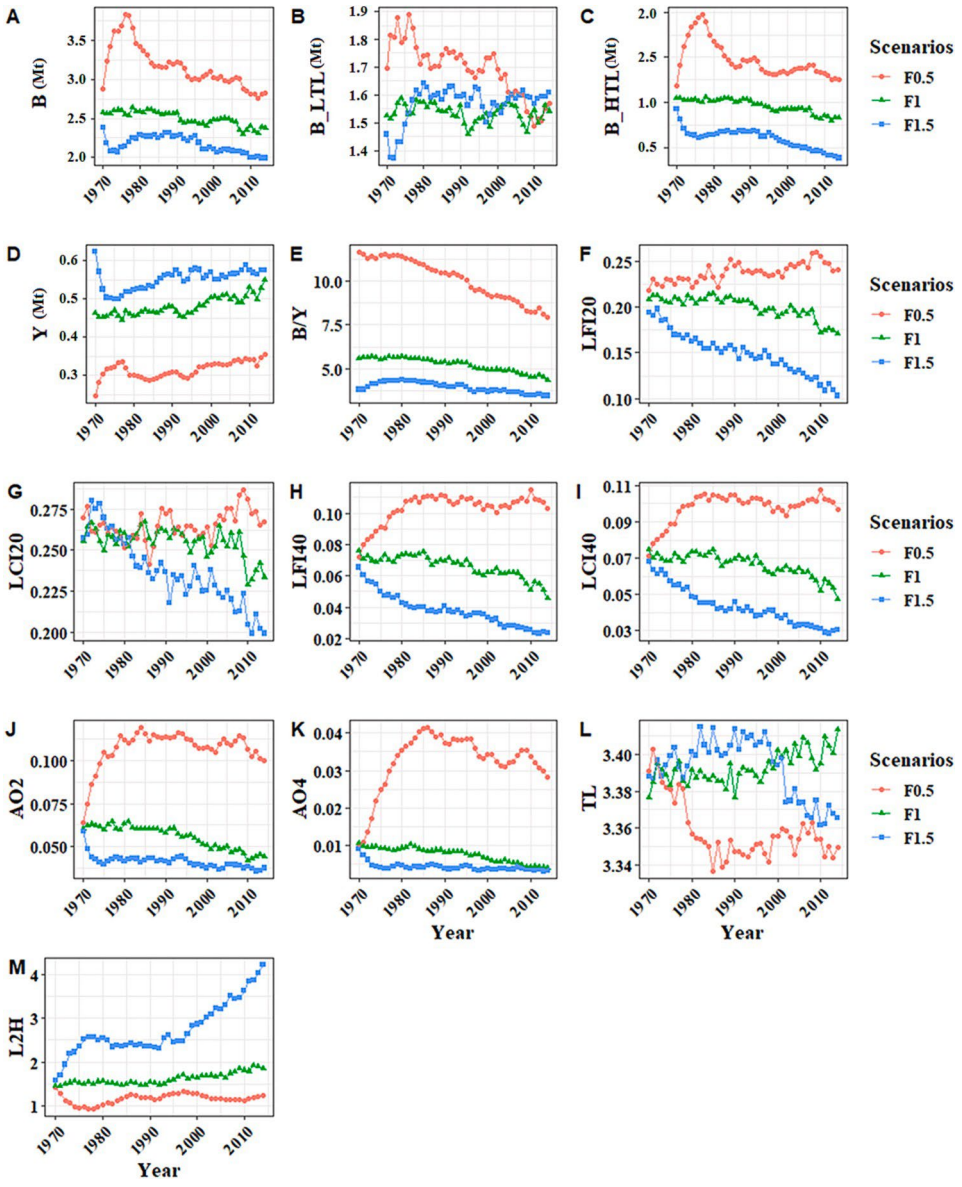

Fig. 7. Changes in ecological indicators under three fishing pressure scenarios (*F0.5*, *F1*, and *F1.5*) during 45 years of simulation in OSMOSE-YS. For ecological indicator codes, see Fig. 6.

4. Discussion

In this study, we have introduced a calibrated OSMOSE-YS model for representing the ecosystem dynamics in the Yellow Sea from 1970 to 2014 and then evaluated the effects of long-term fishing pressure on the structure and function of the Yellow Sea ecosystem. The fishing impacts were analyzed from the species and community perspective in OSMOSE YS. The simulations showed that the biomass of demersal fish continued to decline since the 1970s, while the biomass of pelagic fish and in vertebrates fluctuated periodically. The step changes of ecological in indicators qualitatively matched the historical changes in the Chinese marine fishing industry, especially the decline of catch which mostly came from small, young pelagic fish (Shen and Heino, 2014). This result was consistent with the phenomenon of fisheries-induced evolution, which is now widely found worldwide, where fishery species showed significant changes in phenotypic characteristics (size, weight, and sexual maturity) in response to long-term, sustained, and high-intensity fishing pressure, and where evidence related to the evolution of fish populations in terms of sexual maturity and growth has been found in a wide range of fishery species, such as Atlantic cod (*Gadus morhua*) (Heino et al., 2002; Dieckmann and Heino, 2007). Comparisons among different fishing scenarios indicated that the increase in fishing pressure intensified the trend of biomass reduction and the decreases in body size and maximum ages in the ecosystem. The increase in fishing pressure also caused the biomass-based indicators to decrease sharply, especially *B_HTL*, with potential cascading effects on ecosystem structure and function. As a useful tool to investigate the interactive relationships among multiple species, their spatial pattern and population spatial structure, OSMOSE-YS can be further used to address ecological issues and assist fisheries management in support of the EBFM in the Yellow Sea.

Previous studies showed that with the increase in fishing pressure, ecological dominance in the Yellow Sea ecosystem had gradually changed, and the structure, species diversity, and food web function of fish communities have changed significantly, leading to an increase in the biomass of low trophic level species (Jin and Tang, 1996; Xu et al., 2003; Jin, 2003). The number of species with fast growth rate, small size, short life cycle, and low economic value has significantly increased, gradually occupying a dominant position in the ecosystem structure and food web, while the total biomass of the ecosystem decreased significantly (Dai et al., 2020). Our simulations with the effects of long-term fishing indicated that the biomass, yield, age structure and size structure of the modelled species in OSMOSE-YS have also changed, with different trends across different species. The yield of small pelagic fish generally increased, while their biomasses remained relatively stable. The biomass declines and rapid yield increases for the predatory fish species, e.g. Japanese Spanish mackerel, largehead hairtail, Pacific cod, and chub mackerel, were consistent with findings from previous studies on the impacts of fishing on piscivorous fish (Liu et al., 2021). Largehead hairtail had the highest simulated biomass and yield, consistent with its reported yield (Pauly and Zeller, 2016). Previous studies have indicated that the increase of largehead hairtail yield was caused by the interactive effects of climate change and fishing intensity (Sun et al., 2020a, 2020b; Liu et al., 2021). In this study, we only focused on fishing effects on the Yellow Sea ecosystem, despite the potentially significant effects of climate change, which need to be considered in future work. Of the 13 modelled species, the biomass of yellow striped flounder declined the most, to 4% of initial biomass, followed by the decline of Pacific cod biomass to 15% of initial biomass, and the near population collapse of these two species may be due to complex predator-prey interactions and high fishing mortality (Fig. 2B, E). Japanese anchovy had the highest biomass among the pelagic fish and the second highest among the 13 modelled species; its high biomass could result in part from its predation avoidance due to their vertical distribution.

Considering that age and body length structure of important fish species have changed in the Yellow Sea, we focused on the predicted size and age distribution under three fishing scenarios (Ren et al., 2001; Lin et al., 2006; Mu et al., 2018). Although we found that the long-term fishing pressure drove a decrease in body size and an increase in numbers of young fish (Figs. 6, 7), the patterns of change in size and age structures differed among species under different fishing conditions. In fact, only three modelled species (Japanese anchovy, South American pilchard and southern rough shrimp) had a higher proportion of small individuals under high-fishing condition than under low-fishing condition (Fig. 3). However, these three species are important forage fish, and their trophic levels are the lowest in the ecosystem. Therefore, it is possible that this phenomenon is caused by the dual pressure of fishing pressure and predation (Fig. 5). Moreover, it was found that the proportion of large individual fish in the ecosystem as a whole showed a downward trend under high-fishing condition, but the proportions of small and young individuals increased rapidly and were highest under low-fishing condition (Fig. 7). This may be another reason why the proportions of young fish in the size and age structure among most species were as high as 75% (Fig. 3). Meanwhile, if the model were to be used to further investigate the causes of the reduction in fish size and longevity, the genetic evolution and the bioenergy processes may need to be explicitly considered (Conover et al., 2005; Shan et al., 2012; Liu et al., 2021).

Biomass-based and yield-based indicators can be used to assess the response of marine ecosystems to fishing pressure and promote the transition to ecosystem-based fisheries management (Fu et al., 2020). The total biomass showed an overall downward trend during the whole simulation period, especially from 1990 to 2000, yet the yield showed a continuous increasing trend (Fig. 6A–C). However, *B_HTL* decreased faster than *B_LTL* with increasing fishing, though the latter was 1.5–2 times higher than the former. The indicator *B/Y* in the Yellow Sea ecosystem decreased rapidly after 1990, indicating that the level of fishing exploitation was globally increasing at the ecosystem level. This impacted high trophic level species as shown by the more frequent step changes in *B_HTL*. The trends in biomass-based and yield-based

indicators were further exacerbated with the increase of fishing pressure (Fig. 7A–D). In addition, the continuous rising of fishing engine power had an impact on these indicators, resulting in the decline of biomass and the increase of yield, even under low fishing conditions (Fig. 7A–D). In order to control the fishing intensity and alleviate the pressure on marine fishery resources, China has implemented the "Double-Control" system since 1987, referring to the control of both the total number and the total engine power of marine fishing vessels (Shen and Heino, 2014; Liu et al., 2021). However, this system still needs to be further implemented in some coastal areas to achieve an overall positive effect (Shen and Heino, 2014; Ou and Yu, 2011).

Size-based indicators can reflect the community structure and life history composition of fish; however previous studies pointed out that focusing on large fish indicators only, e.g., *LFI20* or *LFI40*, was not enough to accurately reflect the changes in marine ecosystems (Greenstreet et al., 2012; Fu et al., 2020). Large fish have been the main target of fishing because of their higher economic value. The biomass and yield indicators of large fish, i.e. *LFI20*, *LCI20*, and *LFI40* and *LCI40*, showed similar trends under baseline and high-fishing conditions (Fig. 7F–I). The proportion of large fish biomass kept declining after 1980s under the baseline condition (Fig. 6F, H, Fig. 7F, H). The impacts of increasing fishing engine power were also the reason for the variabilities in the time series of size-based and age-based indicators after the 1980s. With the continuous increase in the scale and intensity of fishery exploitation, coupled with the continuous optimization and upgrading of fishing technology and fishing gear, the fishery resources of the Yellow Sea fishery ecosystem have been in a state of overfishing since the 1980s (Tang et al., 2016). Therefore, we modelled the rapid changes in fishing capacity under the implementation of the "Double-Control" system in this study by incorporating the trend in fishing vessel power into the trend in fishing pressure, thus realizing the impacts of fishing on the dynamics of fish community and phenotypic characteristics. With the increase of fishing pressure, the proportion of large fish in the community decreased significantly (Fig. 7F, H). Likewise, the proportion of large fish in the catch showed a steady downward trend, which indicated that although the increased fishing pressure was targeting large fish, the proportion of large fish in the catch decreased as a result of stocks depletion. The age-based indicators showed that the proportion of elderly individuals decreased with the increasing fishing power of fishing boats since 1995, consistent with a previous study (Fig. 6J, K, Fig. 7J, K; Tang et al., 2016).

For trophic-based indicators, *L2H* increased, indicating that high trophic-level fish were more sensitive to long-term fishing pressure (Fig. 6L, M, Fig. 7L, M). However, the increase of *TL* indicates the change of mean trophic level of modelled species predicted from the calculation of predator-prey relationship. Since ecological indicator *TL* was the average value of mean trophic level of all modelled species, which is not linearly related to biomass, the value of *TL* appeared to increase despite a decrease in *B_HTL* after 1990 under the baseline condition. This indicates that the changes of ecosystem trophic structure can be accurately reflected by comprehensively considering the changes of trophic level and species biomass. Due to the highest *B_LTL* in the early stage of simulation compared with other scenarios and the decrease of large individuals, the mean trophic level is the lowest under low-fishing condition (Fig. 7L). The highest *L2H* under high-fishing condition were due to the rapid reduction of high trophic biomass (Fig. 7M). The results of the study are consistent with the trophic level changes in previous studies of fish feeding at high trophic levels in the Yellow Sea ecosystem, where long-term overfishing led to significant changes in trophic levels of carnivorous fish, as evidenced by the decrease in the proportion of the traditional bait organism Japanese anchovy and the increase in the proportion of shrimp feeding (Jin et al., 2010). The trophic level of the fish community in the Yellow Sea ecosystem continues to decrease due to the change in the composition of the dominant species in the fish community (Zhang et al., 2011). As suggested by studies on "fishing down the food web" that caution is needed in interpreting the assessment of "fishing down marine food webs" based on mean trophic levels, the results of this study found a rapid rise in *L2H* values under high-fishing condition, indicating an increase in lower trophic level species as well as potentially a decrease in biodiversity (Freire and Pauly, 2010; Ding et al., 2017). However, under low fishing conditions, both *B_HTL* and *B_LTL* remained high but TL was lowest, and this "fishing down" during the recovery period may be similar to the low undernourishment in developed country fisheries (Ding et al., 2017).

The calibration of ecosystem models is a crucial step for their credibility due to the complexity of ecosystem models. Although the biomass predicted by OSMOSE-YS is generally lower than the estimates by OCOM, the biomass variation and catch levels of the modelled species are consistent with the previous studies, such as the high yield of largehead hairtail and small yellow croaker (Yan et al., 2014; Zhao et al., 2020; Liu et al., 2021).

Like other ecosystem models, OSMOSE-YS is a simplified representation of a more complex system. Among the modelled species, there are varying degrees of discrepancies between model predictions and observations derived from scientific surveys and literature (Fig. S1). Biomass data used to calibrate the model is estimated by OCOM due to lack of fisheries statistics. However, the estimated biomasses by this assessment method have been used to investigate the decadal variation patterns of fish species in the China Seas (Liu et al., 2021). The fishery data in this study are all based on Chinese fishery without fishery data from other countries in the Yellow Sea, so the spatial grid does not cover the entire Yellow Sea area in the study area setting of the model to avoid inconsistency. The eastern boundary of the study area was the 126° E longitude line, which was only used as the boundary demarcation of the study area because this study focused on the ecological effects of fishing scenarios rather than pursuing the purpose of accurate stock assessment or prediction. The study area that could cover the modelled species was chosen out of the simplicity and idealization of the spatial construction and the actual fishery zoning was not used. In addition, the model simplifies ecological processes and the functioning of the food web. For example, the model uses plankton as food sources for modelled species (i.e. as forcing conditions) without feedback, which implies bottom-up trophic control (Grüss et al., 2015; Halouani et al., 2016; Xing et al.,

2017). Therefore, the process from top predator to primary productivity should be emphasized in future studies, especially in the refinement of food web simulations for the whole ecosystem, not just fisheries eco systems, since the top-down control of predator-prey interactions plays an important role in coastal ecosystems (Östman et al., 2016). Additional groups or species, such as small forage fish and marine mammal species, may eventually be explicitly considered in future versions of OSMOSE-YS when new data become available to improve the food web representation and provide a more accurate picture of ecosystem dynamics. Moreover, the cumulative effects of climate change and fishing on fish stocks have recently been simulated by ecosystem model and ecological individual-based model (Shin et al., 2018; Fu et al., 2020). Since we mainly consider the effects of fishing pressure, and the actual ecological dynamic may be affected by more factors (environment, predation, and other human activities), which may cause the narrower range of the simulated output (biomass and yield) than the observed data. Environmental and fisheries factors, such as changes in temperature and fishing selectivity, can be added to the OSMOSE-YS model to improve the understanding of the Yellow Sea ecosystem, and the combined effects of fishing and climate change.

5. Conclusions

In this study, we illustrated an application of OSMOSE model in the Yellow Sea. The OSMOSE-YS represents the ecosystem dynamics and evaluates the changes at the species and community levels under long time fishing pressure in the Yellow Sea ecosystem. This ecosystem modeling approach was appropriate to provide a realistic representation of the ecosystem dynamics and fishing effects on the structure and functioning of the ecosystem. The increased fishing pressure has led to the continuous increase of the yields for small pelagic fish and the decrease of large-sized commercial fish resources. The results show that the increase in fishing pressure exacerbates the reduction of fish biomass and size. The evaluation of the predicted results of the existing steady state OSMOSE-YS model provides a strong basis for future work. Through reconstructing the population dynamics of all modelled species, we can investigate the effects of long-term fishing pressure on the structure and function of the Yellow Sea ecosystem, examine factors influencing their dynamics considering species interactions, and provide modeling support for Management Strategy Evaluation (MSE) in an ecosystem context (Fu et al., 2017; Grüss et al., 2016).

Declaration of Competing Interest

The authors declare that the research was conducted in the absence of any commercial or financial relationships that could be construed as a potential conflict of interest.

Data availability

Data will be made available on request.

Acknowledgments

This work was supported by the National Natural Science Foundation of China (grant number: 41861134037) and the Research Council of Norway (grant number: 288037). YJS was supported by the Biodiversa and Belmont Forum project SOMBEE. We are extremely grateful to Dr. Caihong Fu (Fisheries and Oceans Canada) for the language editing and advice in improving the manuscript.

Appendix A. Supplementary data

Supplementary data to this article can be found online at https://doi. org/10.1016/j.jmarsys.2023.103946.

References

Christensen, V., Walters, C., 2004. Ecopath with Ecosim: methods, capabilities and limitations. Ecol. Model. 172, 109–139. https://doi.org/10.1016/j.ecolmodel.2003.09.003.

Conover, D.O., Arnott, S.A., Walsh, M.R., Munch, S.B., 2005. Darwinian fishery science: lessons from the Atlantic silverside (*Menidia menidia*). Can. J. Fish. Aquat. Sci. 62, 730–737. https://doi.org/10.1139/F05-069.

Dieckmann, U., Heino, M., 2007. Probabilistic maturation reaction norms: their history, strengths, and limitations. Mar. Ecol. Prog. Ser. 335, 253–269.

Ding, Q., Chen, X., Yu, W., Chen, Y., 2017. An assessment of "fishing down marine food webs" in coastal states during 1950–2010. Acta Oceanol. Sin. 36 (2), 43–50. https://doi.org/10.1007/s13131-017-1003-5.

Duboz, R., Versmisse, D., Travers, M., Ramat, E., Shin, Y.-J., 2010. Application of an evolutionary algorithm to the inverse parameter estimation of an individual-based model. Ecol. Model. 221, 840–849.

Food and Agriculture Organization of the United Nations, 2008. Fisheries Management, FAO Technical Guidelines for Responsible Fisheries. Food and Agriculture Organization of the United Nations, Rome.

Freire, K., Pauly, D., 2010. Fishing down Brazilian marine food webs, with emphasis on the East Brazil large marine ecosystem. Fish. Res. 105 (1), 57–62.

Fu, C., Perry, R., Shin, Y.-J., Schweigert, J., Liu, H., 2013. An ecosystem modeling framework for incorporating climate regime shifts into fisheries management. Prog. Oceanogr. 115, 53–64. https://doi.org/10.1016/j.pocean.2013.03.003.

Froese, R., Pauly, D., 2010. A Global Information System on Fishes, Fishbase. http://www.fishbase.org.

Fu, C., Olsen, N., Taylor, N., Gruss, A., Batten, S., Liu, H., et al., 2017. Spatial and temporal dynamics of predator-prey species interactions off western Canada. ICES J. Mar. Sci. 74, 2107–2119. https://doi.org/10.1093/icesjms/fsx056.

Fu, C., Xu, Y., Guo, C., Olsen, N., Grüss, A., Liu, H., et al., 2020. The cumulative effects of fishing, plankton productivity, and marine mammal consumption in a marine ecosystem. Front. Mar. Sci. 7, 565699

https://doi.org/10.3389/fmars.2020.565699.

Fulton, E., 2010. Approaches to end-to-end ecosystem models. J. Mar. Syst. 81, 171–183. https://doi.org/10.1016/j.jmarsys.2009.12.012.

Fulton, E., Smith, A., Johnson, C., 2004. Effects of spatial resolution on the performance and interpretation of marine ecosystem models. Ecol. Model. 176, 27–42. https://doi.org/10.1016/j.ecolmodel.2003.10.026.

Garcia, S., Zerbi, A., Aliaume, C., Chi, T., 2003. The Ecosystem Approach to Fisheries: Issues, Terminology, Principles, Institution Foundations, Implementation and Outlook. FAO Fisheries Technical Paper 443.

Greenstreet, S.P.R., Fraser, H.M., Rogers, S.I., Trenkel, V.M., Simpson, S.D., Pinnegar, J. K., 2012. Redundancy in metrics describing the composition, structure, and functioning of the North Sea demersal fish community. ICES J. Mar. Sci. 69, 8–22. https://doi.org/10.1093/icesjms/fsr188.

Grüss, A., Schirripa, M., Chagaris, D., Drexler, M., Simons, J., Verley, P., et al., 2015. Evaluation of the trophic structure of the West Florida Shelf in the 2000s using the ecosystem model OSMOSE. J. Mar. Syst. 144, 30–47. https://doi.org/10.1016/j.jmarsys.2014.11.004.

Grüss, A., Harford, W., Schirripa, M., Velez, L., Sagarese, S., Shin, Y.-J., et al., 2016. Management strategy evaluation using the individual-based, multispecies modeling approach OSMOSE. Ecol. Model. 340, 86–105. https://doi.org/10.1016/j.ecolmodel.2016.09.011.

Guo, C., Fu, C., Olsen, N., Xu, Y., Grüss, A., Liu, H., et al., 2019. Incorporating environmental forcing in developing ecosystem-based fisheries management strategies. ICES J. Mar. Sci. 77 (2), 500–514. https://doi.org/10.1093/icesjms/fsz246.

Halouani, G., Ben Rais Lasram, F., Shin, Y.-J., Velez, L., Verley, P., Hattab, T., et al., 2016. Modelling food web structure using an end-to-end approach in the coastal ecosystem of the Gulf of Gabes (Tunisia). Ecol. Model. 339, 45–57. https://doi.org/10.1016/j.ecolmodel.2016.08.008.

Heino, M., Dieckmann, U., Godø, O.R., 2002. Estimation of reaction norms for age and size at maturation with reconstructed immature size distributions: a new technique illustrated by application to Northeast Arctic cod. ICES J. Mar. Sci. 59, 562–575.

Jin, X., 2003. The change of community structure of nekton in the waters off southern Shandong peninsula in spring. J. Fish. China 27, 19–24. https://doi.org/10.3321/j.issn:1000-0615.2003.01.004 (in Chinese).

Jin, X., Tang, Q., 1996. Changes in fish species diversity and dominant species composition in the Yellow Sea. Fish. Res. 26, 337–352. https://doi.org/10.1016/0165-7836(95)00422-X.

Jin, X., Zhang, B., Xue, Y., 2010. The response of the diets of four carnivorous fishes to variations in the Yellow Sea ecosystem. Deep-Sea Res. II Top. Stud. Oceanogr. 57, 996–1000. https://doi.org/10.1016/j.dsr2.2010.02.001.

Levin, P., Fogarty, M., Murawski, S., Fluharty, D., 2009. Integrated ecosystem assessments: developing the scientific basis for ecosystem-based management of the ocean. PLoS Biol. 7, e14 https://doi.org/10.1371/journal.pbio.1000014.

Li, Y., Ma, S., Fu, C., Tian, Y., Li, J., Sun, P., et al., 2021. Appraising the status of fish community structure in the Yellow Sea based on an Indicator-testing framework. Front. Mar. Sci. 8 (646733) https://doi.org/10.3389/fmars.2021.646733.

Lin, L., Zheng, Y., Cheng, J., Liu, Y., Ling, J., 2006. A preliminary study on fishery biology of main commercial fishes surveyed from the bottom trawl fisheries in the East China Sea. Mar. Sci. 30, 21–25. https://doi.org/10.1016/j.ejps.2006.05.004 (in Chinese).

Lin, Q., Jin, X., Zhang, B., 2013. Trophic interactions, ecosystem structure and function in the southern Yellow Sea. Chin. J. Oceanol. Limnol. 1, 13. https://doi.org/10.1007/s00343-013-2013-6.

Liu, D., Tian, Y., Ma, S., Li, J., Sun, P., Ye, Z., et al., 2021. Long-term variability of piscivorous fish in China seas under climate change with implication for fisheries management. Front. Mar. Sci. 8, 581952 https://doi.org/10.3389/fmars.2021.581952.

Ma, M., Chen, Z., Xu, Y., Zhang, K., Yuan, W., Xu, S., 2018. Analysis of structure and energy flow in Jiaozhou Bay ecosystem based on Ecopath model. Chin. J. Ecol. 37, 462–470. https://doi.org/10.13292/j.1000-4890.201802.020 (in Chinese).

Ma, S., Cheng, J., Li, J., Liu, Y., Wan, R., Tian, Y., 2019. Interannual to decadal variability in the catches of small pelagic fishes from China seas and its responses to climatic regime shifts. Deep Sea Res. II Top. Stud. Oceanogr. 159, 112–129. https://doi.org/10.1016/j.dsr2.2018.10.005.

Ma, S., Tian, Y., Fu, C., Yu, H., Li, J., Liu, Y., et al., 2020. Climate-induced nonlinearity in pelagic communities and non- stationary relationships with physical drivers in the Kuroshio ecosystem. Fish Fish. 22, 1–17. https://doi.org/10.1111/faf.12502.

Moullec, F., Barrier, N., Drira, S., Guilhaumon, F., Marsaleix, P., Somot, S., et al., 2019a. An end-to-end model reveals losers and winners in a warming Mediterranean Sea. Front. Mar. Sci. 6, 345. https://doi.org/10.3389/fmars.2019.00345.

Moullec, F., Velez, L., Verley, P., Barrier, N., Ulses, C., Carbonara, P., et al., 2019b. Capturing the big picture of Mediterranean marine biodiversity with an end-to-end model of climate and fishing impacts. Prog. Oceanogr. 178, 102179 https://doi.org/ 10.1016/j.pocean.2019.102179.

Mu, X., Zhang, C., Xu, B., Xue, Y., Tian, Y., Ren, Y., 2018. The fisheries biology of the spawning stock of *Scomberomorus niphonius* in the Bohai and yellow seas. J. Fish. Sci. China 25, 1308–1316. https://doi.org/10.3724/SP.J.1118.2018.17346 (in Chinese).

Oliveros-Ramos, R., Shin, Y.-J., 2016. Calibrar: an R package for fitting complex ecological models. In: ArXiv160303141 Math Q-Bio Stat.

Oliveros-Ramos, R., Verley, P., Echevin, V., Shin, Y.-J., 2017. A sequential approach to calibrate ecosystem models with multiple time series data. Prog. Oceanogr. 151, 227–244. https://doi.org/10.1016/j.pocean.2017.01.002.

Östman, Ö., Eklöf, J., Eriksson, B.K., Olsson, J., Moksnes, Per-Olav, Bergström, Ulf, 2016. Top-down control as important as nutrient enrichment for eutrophication effects in North Atlantic coastal ecosystems. J. Appl. Ecol. 53 (4), 1138–1147.

Otto, S.A., Kadin, M., Casini, M., Torres, M.A., Blenckner, T., 2018. A quantitative framework for selecting and validating food web indicators. Ecol. Indic. 84, 619–631. https://doi.org/10.1016/j.ecolind.2017.05.045.

Ou, H., Yu, C., 2011. The research on effectiveness of fishing vessel double control system. J. Zhejiang Ocean Univ. (Nat. Sci. Ed.) 30 (432–5), 470 (in Chinese).

Pauly, D., Watson, R., 2005. Background and interpretation of the 'Marine Trophic Index' as a measure of biodiversity. Philos. Trans. R. Soc. Lond. B 360, 415–423.

Pauly, D., Zeller, D., 2016. Catch reconstructions reveal that global marine fisheries catches are higher than reported and declining. Nat. Commun. 7, 10244.

Pauly, D., Christensen, V.V., Dalsgaard, J., Froese, R., Torres, F.J., 1998. Fishing down marine food webs. Science 279, 860–863. https://doi.org/10.1126/science.279.5352.860.

Pikitch, E., Santora, C., Babcock, E., Bakun, A., Bonfil, R., Conover, D., et al., 2004. Ecosystem-based fishery management. Science 305, 346–347.

Plagányi, É., 2007. Models for an ecosystem approach to fisheries. In: FAO Fisheries Technical Paper, 477. FAO, Rome, p. 108.

Ren, Y., Gao, T., Liu, Q., Xue, Y., 2001. Study on the population structure and reproduction of *Pseudosciaena plyactis* in southern Yellow Sea. Trans Oceanol. Limnol. 1, 41–46. https://doi.org/10.3969/j.issn.1003-6482.2001.01.008 (in Chinese).

Rodionov, S.N., 2004. A sequential algorithm for testing climate regime shifts. Geophys. Res. Lett. 31, L09204. https://doi.org/10.1029/2004GL019448.

Seidl, R., 2017. To model or not to model, that is no longer the question for ecologists. Ecosystems 20, 1–7. https://doi.org/10.1007/s10021-016-0068-x.

Shan, X.J., Jin, X.S., Zhou, Z.P., Dai, F.Q., 2012. Stock dynamics of *Cleisthenes herzensteini* in the central and southern Yellow Sea. Acta Ecol. Sin. 32, 244–252. https://doi.org/10.1016/j.chnaes.2012.07.010.

Shen, G., Heino, M., 2014. An overview of marine fisheries management in China. Mar. Policy 44, 265–272. https://doi.org/10.1016/j.marpol.2013.09.012.

Shin, Y.J., Cury, P., 2001. Exploring fish community dynamics through size-dependent trophic interactions using a spatialized individual-based model. Aquat. Living Resour. 14, 65–80. https://doi.org/10.1016/S0990-7440(01)01106-8.

Shin, Y.J., Cury, P., 2004. Using an individual-based model of fish assemblages to study the response of size spectra to changes in fishing. Can. J. Fish. Aquat. Sci. 61, 414–431. https://doi.org/10.1139/f03-154.

Shin, Y.J., Bundy, A., Shannon, L.J., Simier, M., Coll, M., Fulton, E.A., et al., 2010. Can simple be useful and reliable? Using ecological indicators to represent and compare the states of marine ecosystems. ICES J. Mar. Sci. 67, 717–731. https://doi.org/10.1093/icesjms/fsp287.

Shin, Y.-J., Houle, J., Akoglu, E., Blanchard, J., Bundy, A., Coll, M., et al., 2018.

The specificity of marine ecological indicators to fishing in the face of environmental change: a multi-model evaluation. Ecol. Indic. 89, 317–326. https://doi.org/10.1016/j.ecolind.2018.01.010.

Sun, P., Chen, Q., Fu, C., Xu, Y., Sun, R., Li, J., et al., 2020a. Latitudinal differences in early growth of largehead hairtail (*Trichiurus japonicus*) in relation to environmental variables. Fish. Oceanogr. 29, 470–483. https://doi.org/10.1111/fog.12490.

Sun, P., Chen, Q., Fu, C., Zhu, W., Li, J., Zhang, C., et al., 2020b. Daily growth of young of-the-year largehead hairtail (*Trichiurus japonicus*) in relation to environmental variables in the East China Sea. J. Mar. Syst. 201, 103243 https://doi.org/10.1016/j.jmarsys.2019.103243.

Sun, R., Sun, P., Fu, C., Liu, G., Liang, Z., Shin, Y.J., et al., 2023. Exploring balanced harvest as a potential strategy for highly exploited multispecies fisheries. ICES J. Mar. Sci. 2023, fsad023. https://doi.org/10.1093/icesjms/fsad023.

Szuwalski, C.S., Burgess, M.G., Costello, C., Gaines, S.D., 2017. High fishery catches through trophic cascades in China. Proc. Natl. Acad. Sci. 114, 717–721. https://doi.org/10.1073/pnas.1612722114.

Szuwalski, C., Jin, X., Shan, X., Clavelle, T., 2020. Marine seafood production via intense exploitation and cultivation in China: costs, benefits, and risks. PLoS One 15, e0227106. https://doi.org/10.1371/journal.pone.0227106.

Tang, Q., Ying, Y., Wu, Q., 2016. The biomass yields and management challenges for the Yellow Sea large marine ecosystem. Environ. Dev. 17, 175–181. https://doi.org/10.1016/j.envdev.2015.06.012.

Thompson, M., Pontalier, H., Spence, M., Pinnegar, J., Greenstreet, S., Moriarty, M., et al., 2020. A feeding guild indicator to assess environmental change impacts on marine ecosystem structure and functioning. J. Appl. Ecol. 57 https://doi.org/10.1111/1365-2664.13662.

Travers, M., Watermeyer, K., Shannon, L.J., Shin, Y.J., 2010. Changes in food web structure under scenarios of overfishing in the southern Benguela: comparison of the Ecosim and OSMOSE modelling approaches. J. Mar. Syst. 79, 101–111.

Travers-Trolet, M., Shin, Y.-J., Field, J., 2014. An end-to-end coupled model ROMS-N2P2Z2D2-OSMOSE of the southern Benguela foodweb: parameterisation, calibration and pattern-oriented validation. Afr. J. Mar. Sci. 36 https://doi.org/10.2989/1814232X.2014.883326.

Wang, Q., Song, J., Zhou, J., Zhao, W., Liu, H., Tang, X., 2016. Temporal evolution of the Yellow Sea ecosystem services (1980–2010). Heliyon 2, e00084. https://doi.org/10.1016/j.heliyon. 2016.e00084.

Wu, Z., Zhang, X., Lozano-Montes, H., Loneragan, N., 2016. Trophic flows, kelp culture and fisheries in the marine ecosystem of an artificial reef zone in the Yellow Sea. Estuar. Coast. Shelf Sci. 182, 86–97. https://doi.org/10.1016/j.ecss.2016.08.021.

Xing, L., Zhang, C., Chen, Y., Shin, Y.-J., Verley, P., Yu, H., et al., 2017. An individual-based model for simulating the ecosystem dynamics of Jiaozhou Bay, China. Ecol. Model. 360, 120–131. https://doi.org/10.1016/j.ecolmodel.2017.06.010.

Xu, B., Jin, X., 2005. Variations in fish community structure during winter in the southern Yellow Sea over the period 1985–2002. Fish. Res. 71, 79–91. https://doi.org/10.1016/j.fishres.2004.07.011.

Xu, B., Jin, X., Liang, Z., 2003. Changes of demersal fish community structure in the Yellow Sea during the autumn. J. Fish. Sci. China 10 (2), 148–154. https://doi.org/10.3321/j.issn:1005-8737.2003.02.013 (in Chinese).

Yan, L., Liu, Z., Zhang, H., Lin, J., Yuan, X., Li, S., 2014. On the evolution of biological characteristic and resources of small yellow croaker. Mar. Fish. 36 (6) (in Chinese).

Yang, S., Jung, H., Lim, D., Li, C., 2003. A review on the provenance discrimination of sediments in the Yellow Sea. Earth Sci. Rev. 63, 93–120. https://doi.org/10.1016/S0012-8252(03)00033-3.

Yu, H., Yu, H., Ito, S.-i., Tian, Y., Wang, H., Liu, Y., et al., 2020. Potential environmental drivers of Japanese anchovy (*Engraulis japonicus*) recruitment in the Yellow Sea. J. Mar. Syst. 212, 103431 https://doi.org/10.1016/j.jmarsys.2020.103431.

Zhang, S., Leng, X., Feng, Y., Ding, C., Yang, Y., Wang, J., et al., 2016. Ecological provinces of spring phytoplankton in the Yellow Sea: species composition. Acta Oceanol. Sin. 35, 114–125. https://doi.org/10.1007/s13131-016-0872-3.

Zhao, X., Cui, L., Liu, X., Situ, J., Chen, E., 2020. Chinese Fishery Statistics. China Agriculture Press, Beijing.

Zhou, S., Punt, A.E., Ye, Y., Ellis, N., Dichmont, C.M., Haddon, M., et al., 2017. Estimating stock depletion level from patterns of catch history. Fish Fish. 18, 742–751. https://doi.org/10.1111/faf.12201.

Zhou, S., Punt, A.E., Smith, A.D.M., Ye, Y., Haddon, M., Dichmont, C.M., et al., 2018. An optimized catch-only assessment method for data poor fisheries. ICES J. Mar. Sci. 75, 964–976. https://doi.org/10.1093/icesjms/fsx226.